BCPT Basic & Clinical Pharmacology & Toxicology

Basic & Clinical Pharmacology & Toxicology, 2017, **120**, 243–249 Doi: 10.1111/bcpt.12675

Use of a Target-Mediated Drug Disposition Model to Predict the Human Pharmacokinetics and Target Occupancy of GC1118, an Anti-epidermal Growth Factor Receptor Antibody

Wan-Su Park[1,2], Seunghoon Han[1,2], Jongtae Lee[1,2], Taegon Hong[3], Jonghwa Won[4], Yangmi Lim[4], Kyuhyun Lee[4], Han Yeul Byun[5] and Dong-Seok Yim[1,2]

[1]Department of Clinical Pharmacology and Therapeutics, Seoul St. Mary's Hospital, Seoul, Korea, [2]PIPET (Pharmacometrics Institute for Practical Education and Training), College of Medicine, The Catholic University of Korea, Seoul, Korea, [3]Department of Clinical Pharmacology, Severance Hospital, Yonsei University College of Medicine, Seoul, Korea, [4]MOGAM Biotechnology Institute, Yongin, Gyeonggi-do, Korea and [5]Green Cross Corp., Yongin, Gyeonggi-do, Korea

(Received 11 July 2016; Accepted 5 September 2016)

Abstract: GC1118 is an anti-epidermal growth factor receptor (EGFR) monoclonal antibody that is currently under clinical development. In this study, the pharmacokinetics (PK) of GC1118 were modelled in monkeys to predict human PK and receptor occupancy (RO) profiles. The serum concentrations of GC1118 and its comparator (cetuximab) were assessed in monkeys with a non-compartmental analysis and a target-mediated drug disposition (TMDD) model after intravenous infusion (3–25 mg/kg) of these drugs. The scaling exponent of the EGFR synthesis rate was determined using a sensitivity analysis. The human cetuximab exposures were simulated by applying different exponents (0.7–1.0) for the EGFR synthesis rate in the allometric monkey PK model. Simulated C_{max} and area under the curve values therein were compared with those previously reported in the literature to find the best exponent for the EGFR synthesis rate in human beings. The TMDD model appropriately described the monkey PK profile, which showed a decrease in clearance (CL; 1.2–0.4 ml/hr/kg) as the dose increased. The exponents for CL (0.75) and volume of distribution (Vd; 1.0) were used for the allometric scaling to predict human PK. The allometric coefficient for the EGFR synthesis rate chosen by the sensitivity analysis was 0.85, and the RO profiles that could not be measured experimentally were estimated based on the predicted concentrations of the total target and the drug–target complex. Our monkey TMDD model successfully predicts human PK and RO profiles of GC1118 and can be used to determine the appropriate dose for a first-in-human study investigating this drug.

Epidermal growth factor receptor (EGFR) is a cell membrane growth factor receptor that is involved in the proliferation and survival of cancer cells [1,2]. EGFR is overexpressed in various types of solid tumours including colorectal, head/neck, breast, lung, prostate, kidney, pancreas, ovary, brain and bladder cancers [3]. Anti-EGFR monoclonal antibodies (mAbs) bind to the extracellular domain of EGFR and compete with endogenous ligands to inhibit the ligand-induced activation of EGFR tyrosine kinase [4]. Currently, two anti-EGFR mAbs, cetuximab and panitumumab, are widely used to treat metastatic colorectal and head/neck cancers [5,6]. Similarly, GC1118 is a fully human IgG_1 mAb that targets the EGFR and is under clinical development for the treatment of colorectal cancer [7].

The prediction of human pharmacokinetics (PK) is an important step for the selection of a safe starting dose and dose escalation schemes in first-in-human (FIH) studies [8]. For mAbs with linear PK characteristics, the human PK can be reasonably predicted based on non-human primate PK data using a simple allometric power model with fixed scaling exponents [9–12]. Although the use of simple allometry is a rational approach for mAbs with linear PK, the principles underlying this method appear to be inadequate for mAbs that exhibit nonlinear PK. The interaction of an antibody with its target often affects the PK properties of the antibody, which in turn influences target-mediated drug disposition (TMDD). Since the TMDD modelling framework was first proposed by Mager *et al.* [13], various approximations have been developed [14–17]. Although several reports have predicted human PK from animal PK for mAbs showing TMDD [15,18–21], there are no general rules for the primate-to-human scaling of parameters related to TMDD [22]. Betts *et al.* [21] and Luu *et al.* [20] used *in vitro* experimental data as fixed values instead of estimating target-related parameters such as target turnover rate, complex turnover rate and the equilibrium binding constant. However, these types of *in vitro* data are not always available at the pre-clinical development stage.

Thus, we evaluated the PK of GC1118 and its comparator (cetuximab) in monkeys and developed a model for predicting human PK by incorporating mechanistic parameters and published information about the comparator. In addition, the human PK data for cetuximab were used to link the target-related parameters between monkeys and human beings and model-predicted target occupancy was calculated for the FIH study design.

Author for correspondence: Dong-Seok Yim, Department of Clinical Pharmacology and Therapeutics, Seoul St. Mary's Hospital, 222 Banpo-daero, Seocho-gu, 06591 Seoul, Korea (fax: +82 2 2258 7876, e-mail yimds@catholic.ac.kr).

Materials and Methods

Overall workflow. After the proposed workflow (fig. 1), the monkey PK data were used to construct the TMDD model, and subsequently, the PK parameters [volume of distribution (Vd) and clearance (CL)] were allometrically scaled to predict human PK. Because there are no general rules for the allometric scaling of target-related parameters, the optimal scaling exponent was chosen by comparing the predicted human PK exposure [C_{max} and area under the curve (AUC)] of the comparator (cetuximab) to data from previous studies [23]. The resulting human TMDD model was used to simulate the PK and receptor occupancy (RO; EGFR saturation) characteristics of various dosage regimens.

Monkey pharmacokinetic data. Monkeys' single dose PK data sets of GC1118 and cetuximab obtained from previous pre-clinical researches sponsored by Green Cross Co. (Gyeonggi-do, Korea) were merged for TMDD modelling. These data consisted of a total of six dosage groups (n = 3–4 per group) for GC1118 (3, 6, 12, or 25 mg/kg) and cetuximab (12 or 25 mg/kg). For all of the dosage groups, male cynomolgus monkeys weighing 2.1–4.0 kg received intravenous (i.v.) administrations of either GC1118 or cetuximab for 1 hr and blood samples were collected from the femoral vein for the PK studies. In the 3, 6 and 25 mg/kg groups, blood samples were obtained prior to the first dose (pre-dose) and at 0 (right after the end of infusion), 0.5, 1, 3, 6, 12, 24, 36, 48, 72, 96, 120, 144, 168, 192, 216, 240, 264, 288, 312, 336, 360, 384 and 408 hr after the i.v. infusion. In the 12 mg/kg group, the sampling time-points were slightly different and occurred at 0 (pre-dose), 0.5 and 1 hr after the start of the i.v. infusion and 10 min. and 0.5, 1, 2, 4, 8, 12, 24, 48, 72, 96, 120, 168, 216, 264, 336 and 408 hr after the i.v. infusion. Serum was separated from whole blood via centrifugation (13,200 rpm for 5 min.), frozen and then stored at −80°C until analysis. The study was conducted at the Korea Institute of Toxicology (Daejeon, Korea) with the approval of the Institutional Animal Care and Use Committee.

Determination of GC1118 and cetuximab concentration in serum. The serum samples were analysed with an enzyme-linked immunosorbent assay (ELISA), and a calibration curve was constructed using SoftMax® Pro software, version 5.2 (Molecular Devices, Sunnyvale, CA, USA) with a four-parameter logistic curve. The lower and upper limits of quantification were 1 and 100 μg/ml,

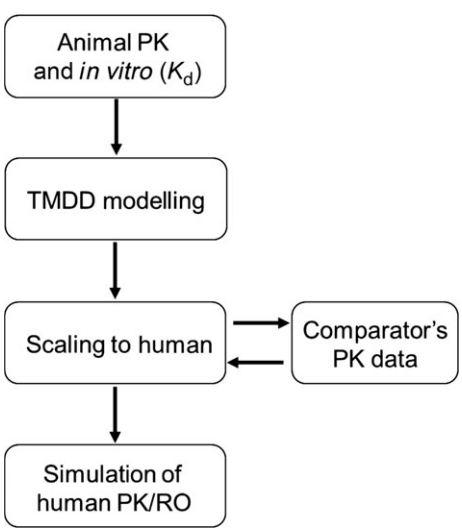

Fig. 1. Workflow for monkey target-mediated drug disposition (TMDD) model and prediction of human pharmacokinetics (PK) and receptor occupancy (RO).

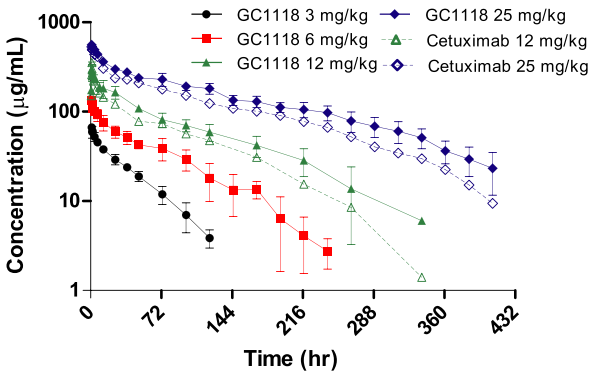

Fig. 2. Mean serum concentration–time profiles of GC1118 and cetuximab after intravenous infusion to cynomolgus monkeys.

respectively. The serum concentration *versus* time profiles of GC1118 in cynomolgus monkeys are provided in fig. 2.

Non-compartmental analysis. A non-compartmental analysis (NCA; Phoenix WinNonlin®, version 6.3, Pharsight Corporation Mountain View, CA, USA) was performed to determine the PK parameters for both GC1118 and cetuximab. The terminal elimination slope (λ_Z) was determined with a least squares regression analysis at the terminal phase, and the AUC_{last}, AUC_{inf}, CL, mean residence time and Vd_{ss} values were determined.

Target-mediated drug disposition (TMDD) model.

QE model building. Parameter estimation was performed with the quasi-equilibrium (QE) approximation of the full TMDD model (fig. 3) [13,15,17] with NONMEM version 7.2 (ICON, Ellicott City, MD, USA). The equations for a two-compartment model where target binding occurs in the tissue (peripheral) compartment were written with respect to the free and total (free + target bound complex) antibodies:

$$\frac{dA}{dt} = \frac{-A \cdot Q}{V_C} + \frac{A_P \cdot Q}{V_P} - \frac{A \cdot CL_A}{V_C}, \quad (1)$$

$$\frac{dTA_P}{dt} = \frac{A \cdot Q}{V_C} - \frac{A_P \cdot Q}{V_P} - \frac{C \cdot CL_C}{V_P}, \quad (2)$$

$$A_P = TA_P - C_P, \quad (3)$$

$$C_P = \frac{K_d \cdot V_P + TA_P + TB_P - \sqrt{(K_d \cdot V_P + TA_P + TB_P)^2 - 4 \cdot TA_P \cdot TB_P}}{2}, \quad (4)$$

$$TB_P = \frac{V_P \cdot RB}{CL_B}, \quad (5)$$

where A is the free antibody in the central compartment, A_P is the free antibody in the peripheral compartment, C_P is the target–antibody complex in the peripheral compartment, TA_P is the total antibodies in the peripheral compartment, TB_P is the total target amount in peripheral compartment, K_d is the equilibrium dissociation constant, RB is the rate of input of binding target (EGFR production rate), V_C is the central compartment volume, V_P is the peripheral compartment volume, CL_A is the CL of free antibody, CL_B is the CL of the binding target (EGFR), CL_C is the CL of the target–antibody complex, and Q is the intercompartmental CL of free antibody between central and peripheral compartment.

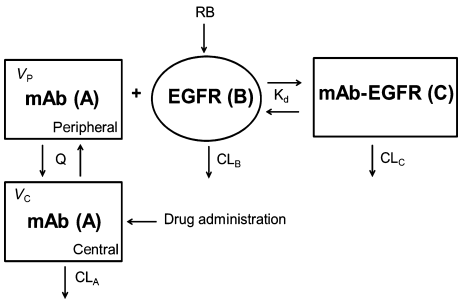

Fig. 3. Structure of the target-mediated drug disposition (TMDD) model. CL_A, clearance of free antibody; Q, intercompartmental clearance; V_C, volume of central compartment; V_P, volume of peripheral compartment; RB, rate of input of binding target; K_d equilibrium binding constant; CL_B, clearance of target; CL_C, clearance of complex; EGFR, epidermal growth factor receptor.

Assumptions used for model building. It was assumed that target binding takes place only in the peripheral compartment (binding in the central compartment is negligible) as exemplified in previous modelling reports [24,25]. The CLs of the unbound target (CL_B) and complex (CL_C) were assumed to be identical because there were no published reports or experimental results regarding their CL. The equilibrium dissociation constant (K_d) was fixed to values obtained from the *in vitro* experiments, and the RO was defined as follows:

$$\mathrm{RO}\,(\%) = \frac{C_P}{\mathrm{TB}_P}. \tag{6}$$

Although the K_d was estimable in the QE model, its relative standard error (RSE) was rather large and the target occupancy predicted thereby was not much different from that predicted by the *in vitro*-fixed K_d, the latter was used (further mentioned in the Discussion section).

Human PK prediction and simulation. To simulate human PK profiles, CL parameters CL_i (CL_A, Q, CL_B) and volume parameters V_i (V_C, V_P) were allometrically scaled using the following equations [26,27]:

$$\mathrm{CL}_{i,\mathrm{human}} = \mathrm{CL}_{i,\mathrm{monkey}} \times \left(\frac{\mathrm{BW}_{\mathrm{human}}}{\mathrm{BW}_{\mathrm{monkey}}}\right)^{0.75}, \tag{7}$$

$$V_{i,\mathrm{human}} = V_{i,\mathrm{monkey}} \times \left(\frac{\mathrm{BW}_{\mathrm{human}}}{\mathrm{BW}_{\mathrm{monkey}}}\right)^{1.0}. \tag{8}$$

The K_d values of the antibodies for the human EGFR used in this step were obtained from the *in vitro* experiments, and typical body-weights of 70 and 3 kg were assumed for human beings and monkeys, respectively.

There is no generally accepted allometric exponent (e.g. 0.75 or 1.0) for target-related parameters such as RB. Thus, a sensitivity analysis was performed to compare the cetuximab C_{max} and AUC values in human beings that were simulated from the allometric PK models (same model parameters except for different RB exponents in each model) with those previously reported in the literature [23]. The allometric exponents for RB that were used for the sensitivity analysis ranged from 0.5 to 1.0 with a step size of 0.05. To select the exponent that provided the simulated exposures of cetuximab (C_{max} and AUC) that were most similar to the observed exposures in patients [23], the predictive performance was evaluated using the percentage prediction error (PPE), root-mean-square error (RMSE), average fold error (AFE) and absolute average fold error (AAFE) that were defined using the following equations, respectively:

$$\mathrm{PPE}\,(\%) = 100 \times \frac{1}{N}\sum \frac{\mathrm{Predicted} - \mathrm{Observed}}{\mathrm{Observed}}, \tag{9}$$

$$\mathrm{RMSE} = \sqrt{\sum \frac{(\mathrm{Predicted} - \mathrm{Observed})^2}{N}}, \tag{10}$$

$$\mathrm{AFE} = 10^{\frac{1}{N}\Sigma\left(\log_{10}\frac{\mathrm{Predicted}}{\mathrm{Observed}}\right)}, \tag{11}$$

$$\mathrm{AAFE} = 10^{\frac{1}{N}\Sigma\left(\left|\log_{10}\frac{\mathrm{Predicted}}{\mathrm{Observed}}\right|\right)}. \tag{12}$$

Subsequently, the one exponent with the best predictive performance was used for the simulation of human PK and RO profiles for GC1118.

Results

Non-compartmental analysis.

NCA results are summarized in table 1. GC1118 showed nonlinear PK over the dose range tested: CL was higher, and half-life was shorter at lower doses. The mean CL decreased from 1.2 to 0.4 ml/hr/kg when the GC1118 dose increased from 3 to 25 mg/kg.

TMDD modelling.

The TMDD model successfully described the serum concentration–time profiles for GC1118 and cetuximab in monkeys. The basic goodness-of-fit plots (fig. 4) and the concentration–time profiles predicted by the final models of GC1118 and cetuximab are illustrated in fig. 5, and the final parameter estimates are summarized in table 2.

Human PK prediction and simulation.

Table 3 provides the model-estimated parameters, except for RB, for the human beings and monkeys that were obtained from the allometric scaling; the exponent for RB was optimized using a sensitivity analysis. The allometric exponent value showing the best predictive performance (PPE, RMSE, AFE and AAFE) was 0.85 for the AUC (table 4), while C_{max} was not influenced by RB. Human PK of GC1118 and its RO profile (saturation of EGFR) after i.v. infusion were simulated using the human PK parameters predicted by the allometric method (fig. 6). Serum concentration and RO *versus* time profiles of cetuximab were simulated after multiple administration of cetuximab according to its approved dosage regimen (http://www.accessdata.fda.gov/drugsatfda_docs/label/2012/125084s0228lbl.pdf). The predicted trough RO of cetuximab at a steady-state was 99.4%, and the dosage regimen of GC1118 that was used for the simulation was adjusted to maintain a similar RO (fig. 7).

Discussion

Overall, the TMDD model successfully described the monkey PK profiles of GC1118 and cetuximab over the tested

Table 1.
Non-compartmental pharmacokinetic parameters of GC1118 and cetuximab after intravenous infusion in monkeys.

	GC1118				Cetuximab	
PK parameters	3 mg/kg[1]	6 mg/kg[1]	12 mg/kg[2]	25 mg/kg[1]	12 mg/kg[2]	25 mg/kg[1]
C_{max} (μg/ml)	66.9 (4.5)	132.8 (16.6)	326 (29.4)	560.9 (37.4)	354.1 (27.4)	533 (66.3)
AUC_{inf} (μg hr/ml)	2451.1 (299.3)	6808.1 (1261.5)	19,931.4 (3824.6)	58,835.5 (7562.7)	14,840 (1733.3)	42,988.7 (5423.1)
CL (ml/hr/kg)	1.2 (0.2)	0.9 (0.2)	0.6 (0.1)	0.4 (0.1)	0.8 (0.1)	0.6 (0.1)
Vd_{ss} (ml/kg)	53.5 (3.5)	58.7 (7.8)	56.1 (5.2)	63.3 (9.1)	64 (6.2)	73 (8.7)
$t_{1/2}$ (hr)	30.2 (4.7)	38.6 (14.7)	64.3 (8.9)	82.6 (48.2)	48.7 (9.3)	52 (41.3)

C_{max}, maximum serum concentration; AUC_{inf}, area under the curve from time zero to infinity; CL, clearance, Vd_{ss}, steady-state volume of distribution; $t_{1/2}$, terminal half-life.
Data are expressed as the mean (standard deviation).
[1]n = 4, [2]n = 3.

Table 2.
Model parameter estimates for GC1118A and cetuximab after intravenous infusion in cynomolgus monkeys.

		Estimate (%RSE)	
Parameters	Description (units)	GC1118	Cetuximab
Structural model			
$CL_A = \theta_1 \cdot (WT/3)^{0.75}$	Clearance of free antibody (ml/hr)	0.975 (8.5)	1.16 (17.2)
$V_C = \theta_2 \cdot (WT/3)$	Volume of central compartment (ml)	141 (2.9)	128 (5.6)
Q	Intercompartmental clearance (ml/hr)	3.87 (19.6)	8.75 (20.2)
$V_P = \theta_4 \cdot (WT/3)^1$	Volume of peripheral compartment (ml)	90.4 (9.4)	126 (5.3)
RB	Rate of input of binding targets (pmol/hr)	284 (8.1)	335 (19.2)
CL_B	Clearance of target (ml/hr)	1.66 (37.8)	2.39 (28.4)
K_d	Equilibrium binding constant (nM)	0.533[2]	7.64[2]
Interindividual variability			
ω_{CLA}	Interindividual variability for CL_A (%)	24.1 (25.1)	25.8 (40.8)
ω_{VC}	Interindividual variability for V_C (%)	9.8 (21.5)	14.1 (35.0)
Residual error			
σ_{prop}	Proportional error (%)	12.9 (12.7)	14.5 (18)

RSE, Relative standard error; WT, body-weight.
[1]WT covariate was only applicable for cetuximab.
[2]K_d values were fixed to *in vitro* monkey K_d value.

Table 3.
Predicted human parameters by allometric scaling.

	Scaling	GC1118		Cetuximab	
Parameters	exponent	Monkey	Human[1]	Monkey	Human[1]
Linear PK parameters					
CL_A (ml/hr)	0.75	0.975	10.4	1.16	12.3
V_C (ml)	1.0	141	3290	128	2987
Q (ml/hr)	0.75	3.87	41.1	8.75	92.9
V_P (ml)	1.0	90.4	2109	126	2940
Target-related parameters					
RB (pmol/hr)	0.85	284	4131	335	4873
CL_B (ml/hr)	0.75	1.66	17.6	2.39	25.4
K_d (nM)	*In vitro*	0.533	0.16[2]	7.64	4.50[2]

CL_A, clearance of free antibody; V_C, volume of central compartment; Q, intercompartmental clearance; V_P volume of peripheral compartment; RB, rate of input of binding targets; CL_B clearance of target; K_d equilibrium binding constant.
[1]$Parameter_{human} = Parameter_{monkey} \times (70/3)^{exponent}$.
[2]*In vitro* human K_d values were used reported in Lim *et al.* [7].

Table 4.
Comparative assessment of exponent values of rate of input of binding target (RB) to predict cetuximab AUC in human beings.

Exponent of RB	PPE (%)	RMSE	AFE	AAFE
0.70	30.2	6630	1.29	1.31
0.75	19.7	5036	1.18	1.25
0.80	9.9	3560	1.08	1.19
0.85	0.6	2466	0.99	1.18
0.90	−7.2	2705	0.91	1.20
0.95	−13.8	3745	0.84	1.27
1.00	−19.6	4970	0.77	1.37

PPE, per cent prediction error; RMSE, root-mean-square error; AFE, average fold error; AAFE, absolute average fold error.

dose range. When the K_d was estimated in this model, the RSE of the estimate was very high (>300%, data not shown), and thus, K_d was fixed to the value obtained from the *in vitro* studies despite its potential to underpredict *in vivo* values [22]. Moreover, the LLOQ of the data used for our modelling (2 μg/ml = 13.3 nM) was much higher than the *in vitro* K_d of GC1118 (0.533 nM), cetuximab (7.64 nM) and their model estimates. Improvement in the model by estimating the K_d instead of using fixed *in vitro* K_d was not significant (OFV decrease 1.1 and 2.7), that implies the K_d estimates are not uniquely identifiable with

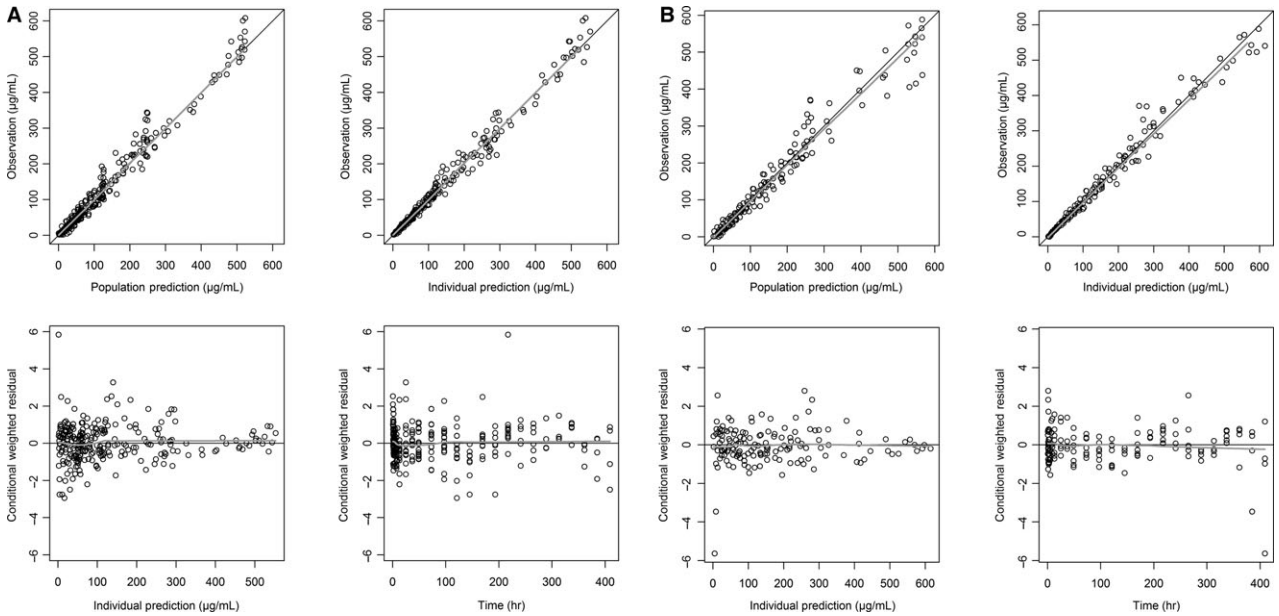

Fig. 4. Basic goodness-of-fit plots for final model of GC1118 (A) and cetuximab (B) in monkey. In the observed *versus* model-predicted concentration plots (upper panels), the solid black and grey line indicate the linear regression fit and identity line, respectively. Whereas in the residual plots (lower panels), grey line was added using the local polynomial regression fitting (Loess smooth) in R.

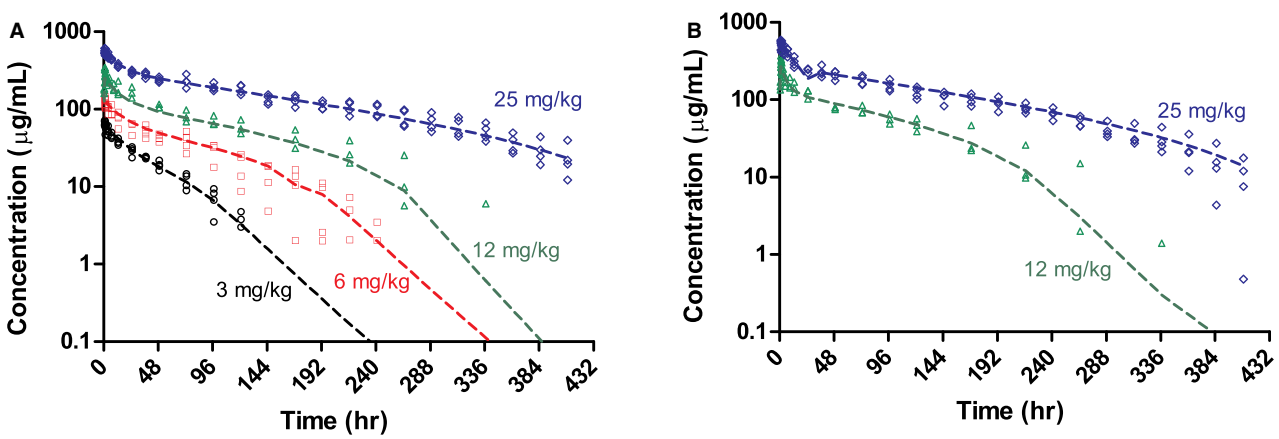

Fig. 5. Median population prediction (lines) and observed concentration (symbols) of GC1118 (A) and cetuximab (B) in monkey.

the current data. At a simulation analysis we carried out for further investigation, the K_d values of 0.1–10 nM were reliably estimable only when concentrations lower than the K_d were included in the simulated data set (results not shown). Thus, using the *in vitro* K_d instead of estimation was inevitable in our QE modelling of mAb. PK and occupancy predicted either by *in vitro* K_d or by estimated K_d were almost identical (see Supporting information).

It was also assumed that the CL of the antibody–target (EGFR) complex (CL_C) was identical to that of the free target CL (CL_B). Based on this assumption, the total target amount remained unchanged, which allowed the model to work without an additional compartment for total target amount in peripheral compartment (TB_P) to describe the change in TB_P over time. The assumption that the CL_B and CL_C values were identical may not reflect the physiological reality in mammals; however, simultaneous estimation of the CL_B, CL_C and TB_P parameters with unbound mAb data only in the QE model in this study was not successful (data not shown).

One challenging aspect of the allometric scaling of human PK parameters from monkey PK parameters was estimating target-specific parameters, such as RB. To the best of our knowledge, the expression rate or turnover rate of EGFR (*in vitro* or *in vivo*) has never been reported. Several reports have indicated that human PK can be predicted with reasonable accuracy using allometrically scaled monkey PK parameters (i.e. CL_A, *Vc*, *Q* or *Vp*) [8–11]. In our study, the exponents for CL_A and *Q* were fixed to 0.75 and that for volume to 1.0 because this was the most commonly cited exponent for metabolic rate [10,26,27]. Thereafter, the performance of the

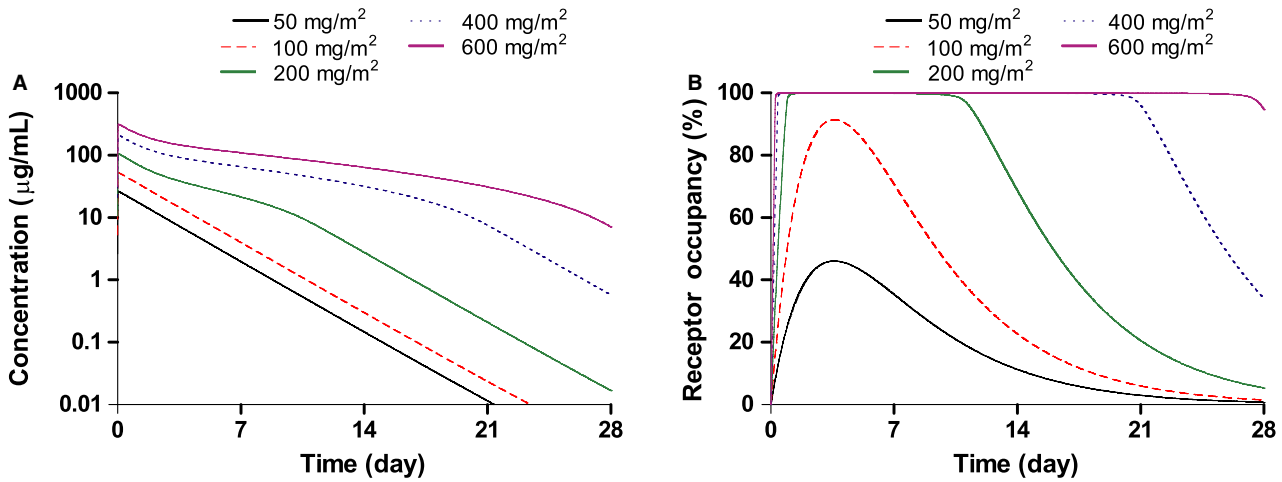

Fig. 6. Simulated serum concentration (A) and receptor occupancy (B) *versus* time profiles of GC1118 after single intravenous infusion of GC1118 at the dose of 50–600 mg/m^2 in human beings.

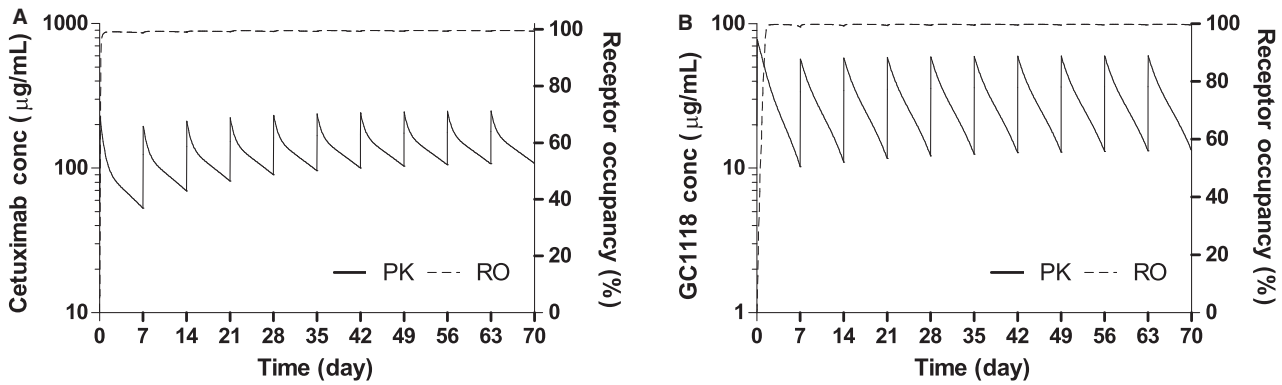

Fig. 7. Simulated serum concentration and receptor occupancy *versus* time profiles of cetuximab (A) and GC1118 (B) after multiple intravenous infusion. Cetuximab was administered an approved therapeutic dosage regimen (loading dose of 400 mg/m^2 and a maintenance weekly dose of 250 mg/m^2). GC1118 was administered new dosage regimen (loading dose of 150 mg/m^2 and a maintenance weekly dose of 90 mg/m^2) to maintain receptor occupancy similar to that of cetuximab.

allometric exponents for RB ranging from 0.7 to 1.0 was compared to select the most appropriate exponent: published cetuximab C_{max} and AUC in patients were compared with the predicted human C_{max} and AUC predicted to find the best exponent for RB. Because patients' PK exposure was used for comparison, the finally selected RB exponent would reflect both the interspecies difference (monkey *versus* human being) and the patient characteristic (possible overexpression of EGFR in patients with cancer unlike the 'normal' monkey). Thus, the allometric exponents obtained after the sensitivity analysis step may be appropriate for the prediction of the GC1118 PK in human patients with cancer. There are several reports that the CL of mAb may be reasonably predicted based on monkey PK data with the scaling exponent of 0.75–0.96 [9–12,28]. When we explored our sensitivity analysis method with varying CL exponents (0.75–0.90) on two human population PK modelling reports of cetuximab [29,30], the best predictive exponents for human cetuximab CL and RB turnover were 0.90 and 0.70, respectively (data not shown). However, we decided to use the fixed exponent as 0.75 for the PK prediction of GC1118 because their population models were Michaelis–Menten [29] or linear [30] that tend to be substantially different from our model (TMDD) in predicting trough concentrations and also because there does not seem to be an agreement on the optimal allometric exponent for mAb CL, yet.

Measuring *in vivo* EGFR occupancy after the infusion of an anti-EGFR mAb is still a challenging task. The model-predicted RO profiles in the present study were simulated using the predicted total target and complex amounts, although neither has been measured experimentally. Despite this uncertainty, the model-predicted RO profiles simulated for the currently approved therapeutic dosage regimens for cetuximab (400 mg/m^2 loading dose followed by 250 mg/m^2 maintenance dose once a week) were near saturation (>99.4%) throughout the dosing interval (fig. 7). This implies that the model-predicted RO profiles were accordant with the expectation under those dosage regimens that the target (EGFR) is fully suppressed (saturated) within the dosing interval. Thus,

in case of developing a mAb against the same target, we find that approaches using the predicted RO to suggest human efficacious doses deserve consideration.

Acknowledgements

This study was funded by Green Cross Corp.

References

1 Martinelli E, De Palma R, Orditura M, De Vita F, Ciardiello F. Anti-epidermal growth factor receptor monoclonal antibodies in cancer therapy. Clin Exp Immunol 2009;**158**:1–9.
2 Amuamuta A, Seifu D. Anti-epidermal growth factor receptor monoclonal antibodies in metastatic colorectal cancer biotherapy: a systematic review. Acad J Cancer Res 2013;**6**:21–8.
3 Yewale C, Baradia D, Vhora I, Patil S, Misra A. Epidermal growth factor receptor targeting in cancer: a review of trends and strategies. Biomaterials 2013;**34**:8690–707.
4 Messersmith WA, Ahnen DJ. Targeting EGFR in colorectal cancer. N Engl J Med 2008;**359**:1834–6.
5 Van Cutsem E, Köhne C-H, Hitre E, Zaluski J, Chang Chien C-R, Makhson A *et al.* Cetuximab and chemotherapy as initial treatment for metastatic colorectal cancer. N Engl J Med 2009;**360**:1408–17.
6 Cohenuram M, Saif MW. Panitumumab the first fully human monoclonal antibody: from the bench to the clinic. Anticancer Drugs 2007;**18**:7–15.
7 Lim Y, Yoo J, Kim MS, Hur M, Lee EH, Hur HS *et al.* GC1118, an anti-EGFR antibody with a distinct binding epitope and superior inhibitory activity against high-affinity EGFR ligands. Mol Cancer Ther 2016;**15**:251–63.
8 Wang J, Iyer S, Fielder PJ, Davis JD, Deng R. Projecting human pharmacokinetics of monoclonal antibodies from nonclinical data: comparative evaluation of prediction approaches in early drug development. Biopharm Drug Dispos 2016;**37**:51–65.
9 Oitate M, Masubuchi N, Ito T, Yabe Y, Karibe T, Aoki T *et al.* Prediction of human pharmacokinetics of therapeutic monoclonal antibodies from simple allometry of monkey data. Drug Metab Pharmacokinet 2011;**26**:423–30.
10 Dong JQ, Salinger DH, Endres CJ, Gibbs JP, Hsu CP, Stouch BJ *et al.* Quantitative prediction of human pharmacokinetics for monoclonal antibodies: retrospective analysis of monkey as a single species for first-in-human prediction. Clin Pharmacokinet 2011;**50**:131–42.
11 Deng R, Iyer S, Theil F-P, Mortensen DL, Fielder PJ, Prabhu S. Projecting human pharmacokinetics of therapeutic antibodies from nonclinical data. mAbs 2011;**3**:61–6.
12 Wang W, Prueksaritanont T. Prediction of human clearance of therapeutic proteins: simple allometric scaling method revisited. Biopharm Drug Dispos 2010;**31**:253–63.
13 Mager DE, Jusko WJ. General pharmacokinetic model for drugs exhibiting target-mediated drug disposition. J Pharmacokinet Pharmacodyn 2001;**28**:507–32.
14 Dua P, Hawkins E, van der Graaf P. A tutorial on Target-Mediated Drug Disposition (TMDD) Models. CPT Pharmacometrics Syst Pharmacol 2015;**4**:324–37.
15 Lowe PJ, Tannenbaum S, Wu K, Lloyd P, Sims J. On setting the first dose in man: quantitating biotherapeutic drug-target binding through pharmacokinetic and pharmacodynamic models. Basic Clin Pharmacol Toxicol 2010;**106**:195–209.
16 Gibiansky L, Gibiansky E, Kakkar T, Ma P. Approximations of the target-mediated drug disposition model and identifiability of model parameters. J Pharmacokinet Pharmacodyn 2008;**35**:573–91.
17 Mager DE, Krzyzanski W. Quasi-equilibrium pharmacokinetic model for drugs exhibiting target-mediated drug disposition. Pharm Res 2005;**22**:1589–96.
18 Li H, Köck K, Wisler Ja, Rees Wa, Prince PJ, Reynhardt KO *et al.* Prediction of clinical pharmacokinetics of AMG 181, a human anti-α 4 β 7 monoclonal antibody for treating inflammatory bowel diseases. Pharmacol Res Perspect 2015;**3**:e00098.
19 Liu X, Ou YC, Zhang J, Ahene A, Clark D, Hsieh SC *et al.* Pharmacokinetics and pharmacodynamics of CD4-anchoring Bi-functional fusion inhibitor in monkeys. Pharm Res 2014;**31**:809–18.
20 Luu KT, Bergqvist S, Chen E, Hu-Lowe D, Kraynov E. A model-based approach to predicting the human pharmacokinetics of a monoclonal antibody exhibiting target-mediated drug disposition. J Pharmacol Exp Ther 2012;**341**:702–8.
21 Betts AM, Clark TH, Yang J, Treadway JL, Li M, Giovanelli MA *et al.* The application of target information and preclinical pharmacokinetic/pharmacodynamic modeling in predicting clinical doses of a Dickkopf-1 antibody for osteoporosis. J Pharmacol Exp Ther 2010;**333**:2–13.
22 Singh AP, Krzyzanski W, Martin SW, Weber G, Betts A, Ahmad A *et al.* Quantitative prediction of human pharmacokinetics for mAbs exhibiting target-mediated disposition. AAPS J 2014;**17**:389–99.
23 Tan AR, Moore DF, Hidalgo M, Doroshow JH, Poplin EA, Goodin S *et al.* Pharmacokinetics of cetuximab after administration of escalating single dosing and weekly fixed dosing in patients with solid tumors. Clin Cancer Res 2006;**12**:6517–22.
24 Lammerts van Bueren JJ, Bleeker WK, Bogh HO, Houtkamp M, Schuurman J, van de Winkel JG *et al.* Effect of target dynamics on pharmacokinetics of a novel therapeutic antibody against the epidermal growth factor receptor: implications for the mechanisms of action. Cancer Res 2006;**66**:7630–8.
25 Cao Y, Jusko WJ. Incorporating target-mediated drug disposition in a minimal physiologically-based pharmacokinetic model for monoclonal antibodies. J Pharmacokinet Pharmacodyn 2014;**41**:375–87.
26 West GB, Enquist BJ, Brown JH. The fourth dimension of life: fractal geometry and allometric scaling of organisms. Science 1999;**284**:1677–9.
27 West GB, Brown JH, Enquist BJ. A general model for the origin of allometric scaling laws in biology. Science 1997;**276**:122–6.
28 Ling J, Zhou H, Jiao Q, Davis HM. Interspecies scaling of therapeutic monoclonal antibodies: initial look. J Clin Pharmacol 2009;**49**:1382–402.
29 Dirks NL, Nolting A, Kovar A, Meibohm B. Population pharmacokinetics of cetuximab in patients with squamous cell carcinoma of the head and neck. J Clin Pharmacol 2008;**48**:267–78.
30 Azzopardi N, Lecomte T, Ternant D, Boisdron-Celle M, Piller F, Morel A *et al.* Cetuximab pharmacokinetics influences progression-free survival of metastatic colorectal cancer patients. Clin Cancer Res 2011;**17**:6329–37.

Supporting Information

Additional Supporting Information may be found online in the supporting information tab for this article:

Data S1. Berkeley Madonna code for the final PK (quasi-equilibrium) model.

Figure S1. Example simulation graph using the code.

Table S1. Final parameter estimates of GC1118 and Cetuximab.